Article

Not peer-reviewed version

The Influence of DOC on the Migration Forms of Elements and Their Sedimentation From River Waters at an Exploited Diamond Deposit (NW Russia)

Alexander I Malov * , Evgeniya S Sidkina , Elena V Cherkasova

Posted Date: 4 May 2023

doi: 10.20944/preprints202305.0238.v1

Keywords: wastewater; river water; groundwater; migration species; bottom sediments; modeling doi:10.20944/preprints202305.0238.v1

Article

The Influence of DOC on the Migration Forms of Elements and Their Sedimentation From River Waters at an Exploited Diamond Deposit (NW Russia)

Alexander I. Malov [1,*] Evgeniya S. Sidkina [2] and Elena V. Cherkasova [2]

[1] N. Laverov Federal Center for Integrated Arctic Research of the Ural Branch of the Russian Academy of Sciences, 20 Nikolsky Ave., 163020 Arkhangelsk, Russia
[2] Vernadsky Institute of Geochemistry and Analytical Chemistry of the Russian Academy of Sciences, 19 Kosygin st, 119991 Moscow, Russia; SidkinaES@yandex.ru (E.S.S.); wri-lab@geokhi.ru (E.V.C.)
* Correspondence: malovai@yandex.ru

Abstract: The development of mineral deposits causes changes that are comparable to natural exogenous geological processes, and in local areas of intensive mining activity prevail over them. In this article, a diamond deposit is selected, developed by quarries of great depth, and a forecast is made of the impact of drainage water discharge on changes in the composition of surface water and bottom sediments during the entire period of development of the deposit. Modeling was performed according to various scenarios, taking into account changes in the total dissolved solids of groundwater from 0.5 to 21.7 g/kg H_2O. Thermodynamic calculations were carried out using the HCh software package. The role of dissolved organic carbon in the migration of chemical elements and the effect of DOC on the precipitation of chemical elements from mixing solutions is given. It has been established that fulvic acid completely binds to Fe in the $Fe(OH)_2FA^-$ complex in all types of natural waters and under all mixing scenarios. With humic acid, such a sharp competitive complex formation does not occur. It is distributed among the various elements more evenly. It was determined that the mass of precipitating iron in the presence of DOC decreases by 18-27%, and its precipitation in winter is more intense. In contrast to Fe, precipitation of Ca, Mg, and C from solution with DOC is higher in summer, and there are more of them in solution in winter. This study contributed to a better understanding of the behavior of heavy metals in surface waters and sediments under anthropogenic pressures in order to improve the sustainable management of water resources in the face of anthropogenic activities.

Keywords: wastewater; river water; groundwater; migration species; bottom sediments; modeling

1. Introduction

The development of mineral deposits causes changes that are comparable to natural exogenous geological processes, and in local areas of intensive mining activity prevail over them. The resulting technogenesis initiates an aggravation of the course of destructive geological processes and introduces substances, forces and processes into the biosphere that change and disrupt its equilibrium functioning and the closed nature of the biotic cycle [1,2]. The strongest impact on the natural landscape is exerted by open pit mining of minerals, the area of which is constantly growing. Mining developments lead to the emergence of geochemical anomalies of anthropogenic origin, when elevated concentrations of individual elements and their compounds are observed in mining areas [3–5]. They are especially pronounced in surface waters and bottom sediments of streams and reservoirs, into which wastewater from mining enterprises that extract coal and iron ores is discharged [6–12].

Mining operations at diamond deposits are no exception. However, due to the much smaller distribution of such deposits in the world and some limited and (or) closed information, there are relatively few scientific publications on their impact on the ecological state of water resources and their exploitation is more often analyzed in a socio-economic context [13–17]. At the same time, they are characterized by specific features associated, among other things, with the mineralogical composition of ultramafic kimberlite rocks, as shown by our studies at a diamond deposit in northwestern Russia [18,19] (Figure 1).

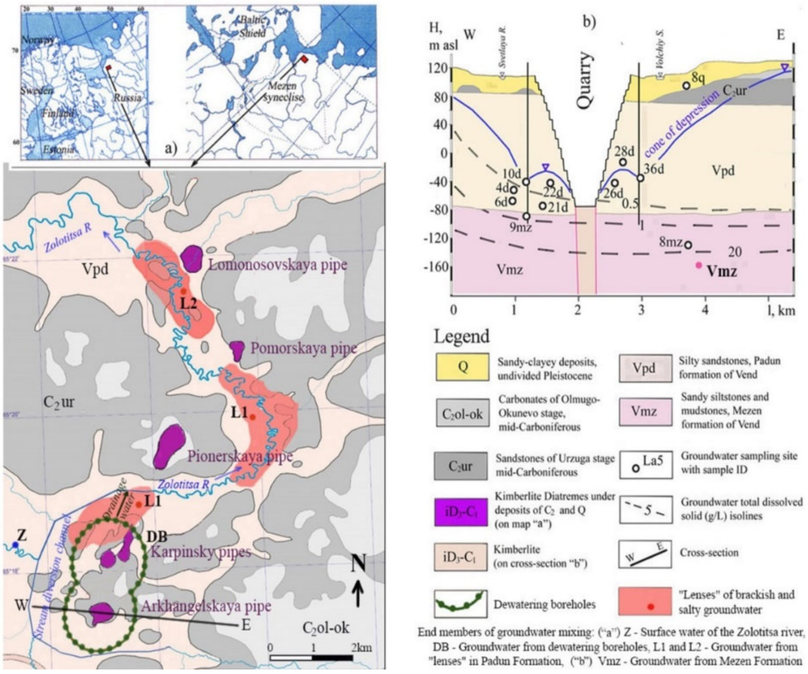

Figure 1. (**a**) General location of study site showing end members involved in mixing of surface waters of Zolotitsa River (Z) with fresh groundwater pumped from dewatering boreholes (DB); brackish and salty groundwater pumped from "lenses" in Vendian Padun Formation (L1 and L2); and (**b**) salty groundwater pumped from Vendian Mezen Formation (Vmz).

The kimberlites of this deposit are characterized by very strong alteration associated with chemical weathering of the main rock-forming mineral olivine. This weathering took place both at the stage of intrusion of high-temperature kimberlite melt into the flooded sedimentary cover, and during further water-rock interaction during 460 million years [20]. As a result, the overwhelming volume of kimberlite pipes is represented by a clay mineral from the montmorillonite group, saponite. When diamonds are extracted at processing plants, saponite is completely washed out with water, and in the form of a colloidal suspension is removed to the filtration fields in the swamp massif, on which it partially settles, and partially penetrates into the river and settles there. Possessing high sorption properties, it sorbs heavy metals entering the river with drainage water discharged into it from dewatering boreholes (DB) (Figure 1a).

In addition, in the course of geological exploration, it was found that in the valley of the Zolotitsa River, saline water is being discharged from deep aquifers. Currently, they are located in the form of saline lenses L1 and L2 in the aquifer of the Vendian Padun Formation (Vpd) sandstones (Figure 1a) and have already begun to pull up to the dewatering boreholes from lens L1 due to the cone of depression formed around the DB (Figure 1b). In the future, the open pit field will expand to the north, and the process of drainage water salinization will be intensified due to lens L2, as well as due to the upwelling of saline water from the deep horizon of sandstones of the Vendian Mezen Formation (Vmz) (Figure 1b).

Salinization and (or) pollution of the Zolotitsa River is unacceptable due to its special fish protection status [21], therefore, a detailed analysis of the formation of the chemical composition of surface water and bottom sediments in the process of mining operations at the deposit is necessary until they are fully completed. The water of the Zolotitsa River, like most of the rivers of the Northern region, contains a high concentration of dissolved organic carbon (DOC), which plays a significant role in the behavior of some chemical elements, including potentially toxic ones. When considering the issues of mixing natural waters of various types, it is necessary to take into account the presence of organic matter in the system for a correct understanding of the forms of occurrence of chemical elements and the possibility of secondary mineral formation. Thus, in the formation of complex particles of metals with organic matter, it is possible to block the formation of secondary mineral phases. In other words, the presence of DOC in water changes the functioning of geochemical barriers [22–24].

Earlier, we have already considered this problem [25] using the calculation of the equilibrium composition of mixing solutions. Our task was to estimate the maximum possible scale of sedimentation of secondary minerals from discharged waters. However, we did not take into account organic matter in the model, which led to insufficiently good comparability with natural observations in terms of elements that have a strong affinity for organic matter. Therefore, in this work, we carried out thermodynamic calculations taking into account DOC. The calculations were carried out using the HCh software package [26]. The main tasks were the following: i) determination of the migration forms of chemical elements both in the initial natural surface and groundwater, and under various scenarios of changes in the composition of surface waters with the further development of mining operations; ii) assessment of the role of DOC in the intensity of precipitation of chemical elements from mixing solutions of drainage and surface waters.

The following scenarios of river surface water mixing were considered: (i) with fresh water DB, ii) taking into account the inflow of saline water to DB from lens L1, (iii) taking into account the inflow of saline water to DB from lens L2, (iv) taking into account the inflow of saline water to DB from the aquifer of the Vendian Mezen Formation (Vmz).

2. Materials and Methods

Modeling of changes in the composition of water in the Zolotitsa River (Z) was carried out when fresh drainage groundwater was discharged into it from a DB system according to the following scenarios: 1) Mixing DB - Z in a ratio of 2:1; 2) the same, when brackish waters are drawn to the DB from the lens in the aquifer complex of deposits of the Vendian Padunskaya suite (L1) in a ratio of 1:3; 3) the same, when saline water is pulled up to the DB from the lens in the aquifer complex of deposits of the Vendian Padunskaya suite (L2) in a ratio of 1:3; 4-6) the same, when saline waters are drawn to the DB from the underlying aquifer of the Vendian Mezen Formation (Vmz) in the ratios of 1:100, 4:100 and 7:100. The ratio 7:100 is the ratio of the water conductivities of the aquifers of the Mezen and Padun suites. Theoretically, in this ratio, the maximum flow in the steady state can be carried out.

Thermodynamic calculations were carried out using the HCh software package (Shvarov, 1999). The system consisted of 24 chemical elements: O, H, C, S, Cl, Ca, Mg, Na, K, Fe, Al, Mn, Ni, Cu, Zn, Cd, Cr, Sr, Pb, Mo, As, U , FA (fulvic acid), HA (humic acid). FA and HA are introduced into the HCh program as new independent elements. To take into account the complex formation of chemical elements with organic ligands, the Unitherm database was supplemented with the corresponding free energies. Free energies FA^{2-} and HA^{-} are taken equal to zero. Free energies of formation of complexes with organic ligands are calculated by the equation:

$$G^{0*}_{fMeA} = G^{0}_{fMe^{m+}} - RTlnK_{ef},$$

where $\boldsymbol{G^{0*}_{fMeA}}$is the free energy of complex formation with an organic anion; $\boldsymbol{G^{0}_{fMe^{m+}}}$ is the free energy of the metal ion; *R* is the gas constant; *T* is temperature (298.15 K); $\boldsymbol{K_{ef}}$ is the effective stability constant [27]. The effective stability constants from [28–38] were used to calculate the free energies of formation of complexes with fulvic and humic acids. A complete list of aqueous species is given in Table 1.

Accounting for organic matter in computer simulations has been successfully used in other objects [39–41].

Table 1. Aqueous species, taken into account in simulation.

H_2O
H^+
OH^-
H_2 (aq)
O_2 (aq)
Al^{3+}
$AlOH^{2+}$
AlO^+
$AlOOH^0$
AlO_2^-
$HAsO_2^0$
AsO_2^-
$HAsO_3^{2-}$
AsO_4^{3-}
$HAsO_4^{2-}$
$H_2AsO_4^-$
$H_3AsO_4^0$
CO_3^{2-}
HCO_3^-
CO_2 (aq)
Ca^{2+}
$CaOH^+$
$CaCl^+$
$CaCl_2^0$
$CaSO_4^0$
$CaCO_3^0$
$CaHCO_3^+$
Cd^{2+}
$CdOH^+$
CdO^0
$HCdO_2^-$
CdO_2^{2-}
$CdCl^+$
$CdCl_2^0$
$CdCl_3^-$
$CdCl_4^{2-}$
$Cd(HSO_4)_2^0$
$CdHCO_3^+$
Cl^-
HCl^0
Cr^{2+}
Cr^{3+}
CrO^+
$CrOH^{2+}$
$HCrO_2^0$
CrO_2^-
CrO_4^{2-}
$HCrO_4^-$
$Cr_2O_7^{2-}$
Cu^+
$CuOH^0$
$CuCl^0$
$CuCl_2^-$
$CuCl_3^{2-}$
$CuHCO_3^0$
Cu^{2+}
$CuOH^+$
CuO^0
$HCuO_2^-$
CuO_2^{2-}
$CuCl^+$
$CuCl_2^0$
$CuCl_3^-$
$CuCl_4^{2-}$
$CuSO_4^0$
$CuHSO_4^+$
$CuCO_3^0$
$CuHCO_3^+$
Fe^{2+}
$FeOH^+$
FeO^0
$HFeO_2^-$
$FeCl^+$
$FeCl_2^0$
$FeSO_4^0$
$FeCO_3^0$
Fe^{3+}
$FeOH^{2+}$
FeO^+
$HFeO_2^0$
FeO_2^-
$FeCl^{2+}$
$FeCl_2^+$
$FeCl_3^0$
$FeSO_4^+$
$FeHSO_4^{2+}$
K^+
KOH^0
KCl^0
KSO_4^-
$KHSO_4^0$
KCO_3^-
$KHCO_3^0$
Mg^{2+}
$MgOH^+$
$MgCl^+$
$MgCl_2^0$
$MgSO_4^0$
$MgCO_3^0$
$MgHCO_3^+$
Mn^{2+}
$MnOH^+$
MnO^0
$HMnO_2^-$
MnO_2^{2-}
$MnCl^+$
$MnCl_2^0$
$MnSO_4^0$
$MnHCO_3^+$
Mn^{3+}
MnO_4^-
MnO_4^{2-}
MoO_4^{2-}
$HMoO_4^-$
Na^+
$NaOH^0$
$NaCl^0$
$NaSO_4^-$
$NaCO_3^-$
$NaHCO_3^0$
Ni^{2+}
$NiOH^+$
NiO^0
$HNiO_2^-$
NiO_2^{2-}
$NiCl^+$
Pb^{2+}
$PbOH^+$
PbO^0
$HPbO_2^-$
$PbCl^+$
$PbCl_2^0$
$PbCl_3^-$
$PbCl_4^{2-}$
$PbSO_4^0$
$PbHSO_4^+$
$PbCO_3^0$
$PbHCO_3^+$
SO_4^{2-}
HSO_4^-
Sr^{2+}
$SrOH^+$
$SrCl^+$
$SrCl_2^0$
$SrSO_4^0$
$SrCO_3^0$
$SrHCO_3^+$
U^{3+}
UOH^{2+}
UO^+
HUO_2^0
U^{4+}
UOH^{3+}
UO^{2+}
HUO_2^+
UO_2^0
HUO_3^-
UCl^{3+}
UCl_2^{2+}
USO_4^{2+}
$UHSO_4^{3+}$
UCO_3^{2+}
$UHCO_3^{3+}$
UO_2^+
UO_2OH^0
UO_3^-
UO_2Cl^0
$UO_2Cl_2^-$
$UO_2HCO_3^0$
$UO_2(HCO_3)_2^-$
UO_2^{2+}
UO_2OH^+
$U_2O_4(OH)_2^{2-}$
$UO_2(OH)_2^0$
$UO_2SO_4^0$
$UO_2(SO_4)_2^{2-}$
$UO_2CO_3^0$
$UO_2(CO_3)_2^{2-}$
UO_3^0
UO_4^{2-}
HUO_4^-
Zn^{2+}
$ZnOH^+$
ZnO^0
$HZnO_2^-$
ZnO_2^{2-}
$ZnCl^+$
$ZnCl_2^0$
$ZnCl_3^-$
$ZnCl_4^{2-}$
$ZnSO_4^0$
$ZnHSO_4^+$
$ZnCO_3^0$
$ZnHCO_3^+$
FA^{2-}
HFA^-
$CaFA^0$
$MgFA^0$
$FeFA^0$
$FeFA^+$
$FeOHFA^0$
$Fe(OH)_2FA^-$
$AlFA^+$
$CuFA^0$
$Cu(OH)_2FA^{2-}$
$ZnFA^0$
$PbFA^0$
HA^-
HHA^0
$CaHA^+$
$MgHA^+$
$FeHA_3^0$
$CuHA_2^0$
$CuHA^+$
$ZnHA^+$
$PbHA_2^0$
$PbHA^+$
H_2FA^0
$MnFA^0$
$CdFA^0$
$MnHA^+$
$CdHA_2^0$
MoO_2HA^+
$MoO_2HA_2^0$
UO_2FA^0
$UO_2FA_2^{2-}$
UO_2HA^+
$UO_2HA_2^0$
$SrFA^0$
$SrHu^+$
$Sr(HA)_2^0$
$CrFA^+$
$CrHu^{+2}$
$Cr(OH)FA^0$
$NiFA^0$
$NiHA^+$

The model took into account the possibility of formation of the following minerals: dolomite, gibbsite, goethite, pyrolusite, ankerite, malachite, siderite, zincite. In addition to the above phases, the model took into account the possibility of the formation of calcite containing strontium, zinc, lead, and manganese. In other words, it is a solid solution of variable composition.

The chemical compositions of water samples were taken as initial data (Table 2). Procedures related to their obtaining are described in [18]. All of the water samples were filtered through 0.45 μm acetate cellulose in the field. The solutions that were filtered for cation and trace element analyses were acidified with double-distilled HNO_3 ($pH < 2$); the samples for anion analysis were not acidified. The water temperature, pH, and Eh were measured in the field using portable HANNA instruments with uncertainties of 0.1 °C, 0.05 pH units, and 0.1 mV, respectively. The calcium, magnesium, sodium, and potassium concentrations were determined with an uncertainty of 1-2% by using an atomic absorption spectrometer (AAS) (Perkin-Elmer 5100 PC). The alkalinity was measured by potentiometric titration with HCl using an automated titrator (Metrohm 716 DMS Titrino) and using the Gran method (detection limit 10^{-5} M, uncertainty at ≥0.5 mmol/l 1-3%, at <0.5 mmol/l 7%. The major anion concentrations (Cl^-, SO_4^{2-}) were measured by ion chromatography (HPLC, Dionex ICS 2000) with an uncertainty of 2%. Major and trace elements were determined without pre-concentration by inductively coupled plasma mass spectrometry (ICP-MS) (Agilent 7500ce) at GET, Toulouse, France. Good agreement (≤ 10%) between measured and certified U concentration in a certified river water sample (SLRS-5) was achieved. DOC was measured using a Shimadzu TOC 6000 with an uncertainty of 5%. The contents of fulvic and humic acids were calculated from the DOC concentration according to the method proposed in [27]. According to the method, it is assumed that carbon is 40% of fulvic and humic acids, and their ratio is 10:1.

Table 2. Initial compositions of surface water and groundwater, taken in modeling their mixing.

	ZS [1]	**ZW** [1]	**DB**	**L1**	**L2**	**Vmz**
T°C	14	0.6	4.5	4.9	5.7	6.9
pH	7.5	7.3	8.6	7.9	7.7	8.3
Eh, mV	281	120	65	-22	-38	-80
			mg/kg H_2O			
Fulvic acids (FA)	28.2	16.1	3.03	7.55	2.92	2.56
Humic acids (HA)	1.57	0.9	0.17	0.42	0.16	0.14
O_2	10.3	6.1	1.7	0	1.2	0
Na	13.3	13.3	101.3	792	1960	5374
Mg	3.12	3.12	9.86	48.4	298	484
K	0.8	0.8	4.24	6.88	33.6	52.8
Ca	6.06	6.06	17.6	49.6	495	1804
Cl	8.22	8.22	73	1009	3034	11,502
HCO_3^-	48.8	48.8	211	325	255	19.8
SO_4^{2-}	4.2	4.2	33.6	292	2,323	2,326
TDS	87.1	87.1	455	2528	8418	21,664
			µg/kg H_2O			
Al	57.2	57.2	7	25.2	34	187
Cr	0.37	0.37	0.63	0.99	1.54	18.5
Mn	13.4	13.4	12.5	78.6	814	3,153
Fe	339	339	35.1	1341	1872	6564
Ni	0.3	0.3	0.11	0.82	1.86	2.31
Cu	0.25	0.25	0.16	1.2	1.84	0.29
Zn	5.13	5.13	2.17	14.8	23.8	49.2
As	0.5	0.5	0.6	0.39	0.36	1.22
Sr	64.3	64.3	168	671	12,301	38,594
Mo	0.37	0.37	2.7	18.1	3.46	9.3

Cd	0.0028	0.0028	0.0044	0.04	0.04	0.035
Pb	0.106	0.106	0.045	1.47	2.02	0.06
U	0.59	0.59	6.78	1.57	15.2	0.15

[1] S – summer; W – Winter;.

3. Results and Discussion

3.1. Organic and Inorganic Aqueous Species of Elements in the Natural Waters of the Study Area

The results of calculations of the forms of occurrence of chemical elements in the natural waters of the study area are given in Table 3.

Table 3. Simulated dominant aqueous species of chemical elements in natural waters at the study area (mol %).

Aqueous species	ZS	ZW	DB	L1	L2	Vmz	Aqueous species	ZS	ZW	DB	L1	L2	Vmz
		FA					$CuCl_2^-$	0	0	0	80.86	57.38	24.38
$Fe(OH)_2 FA^-$	100	100	100	100	100	100	$CuCl_3^{2-}$	0	0	0	17.60	42.26	75.58
		HA					Cu^{2+}	4.77	10.17	0.77	0	0	0
HA^-	40.67	40.67	34.49	12.91	2.27	0.86	$CuOH^+$	1.99	2.82	0.55	0	0	0
HHA^0	0.01	0.01	0	0.01	0	0	CuO^0	12.86	11.97	7.34	0	0	0
$MgHA^+$	15.02	15.02	14.72	32.27	25.33	14.49	$CuCl^+$	0	0.01	0	0	0	0
$CaHA^+$	43.94	43.94	50.74	54.64	72.29	84.37	$CuSO_4^0$	0	0.06	0.02	0	0	0
$MnHA^+$	0	0	0	0.12	0.08	0.22	$CuCO_3^0$	80.19	74.63	91.31	0	0	0
$CuHA^+$	0.01	0.01	0	0	0	0.02	$CuHCO_3^+$	0.02	0.03	0.01	0	0	0
$ZnHA^+$	0.33	0.33	0.05	0.04	0.02	0	$Cu(OH)_2 FA^{2-}$	0	0	0	0	0	0
$SrHA^+$	0.01	0.01	0	0,01	0.01	0.04	$CuHA^+$	0.14	0.31	0	0	0	0
$PbHA^+$	0	0	0	0	0	0			**Zn**				
		Mg					Zn^{2+}	70.70	80.12	44.46	76.64	73.22	83.25
Mg^{2+}	98.49	98.82	93.92	86.50	71.95	78.88	$ZnOH^+$	19.02	14.32	16.01	2.70	0.82	0.65
$MgOH^+$	0.01	0	0.01	0	0	0	ZnO^0	0.07	0.03	0.11	0	0	0
$MgCl^+$	0.01	0.01	0.11	1.00	1.8	5.87	$HZnO_2^-$	0	0	0	0	0	3,62
$MgCl_2^0$	0	0	0	0.05	0.23	2.49	$ZnCl^+$	0.01	0.01	0.03	0.52	1.07	0.85
$MgSO_4^0$	0.55	0.59	2.89	9.32	25.05	12.7	$ZnCl_2^0$	0	0	0	0.02	0.08	0.21
$MgCO_3^0$	0.18	0.08	1.04	0.17	0.02	0	$ZnCl_3^-$	0	0	0		0.01	0.05
$Mg HCO_3^+$	0.76	0.5	2.04	2.96	0.95	0.06	$ZnHS^+$	0	0	0	0.02	0.01	0.01
$MgHA^+$	0	0	0	0	0	0	$ZnSO_4^0$	0.41	0,49	1,38	7.97	23.06	11.27
		Ca					$ZnCO_3^0$	9.33	4.61	37.52	10.86	1.29	0.06
Ca^{2+}	98.49	98.93	94.05	89.96	81.24	88.71	$ZnHCO_3^+$	0.30	0.23	0.48	1.26	0.44	0.03
$CaCl^+$	0.01	0.01	0.06	0.57	1.05	3.19	$ZnHA^+$	0.16	0.19	0.01	0.01	0	0
$CaCl_2^0$	0	0	0	0.01	0.03	0.3			**As**				
$CaSO_4^0$	0.36	0.38	1.93	6.15	16.68	7.74	AsO_4^{3-}	0.02	0.01	0.06	0	0	0

$CaCO_3^0$	0.35	0.15	1.87	0.30	0.03	0
$CaHCO_3^+$	0.78	0.52	2.09	3.01	0.97	0.06
$CaHA^+$	0.01	0.01	0	0	0	0
		Al				
Al^{3+}	0	0	0	0	0.02	0.07
$AlOH^{2+}$	0	0	0	0.02	0.38	0.9
AlO^+	0.03	0.07	0.01	0.38	2.13	3.14
$AlOOH^0$	5.49	8.22	2.29	14.60	28.71	32.13
AlO_2^-	94.48	91.71	97.7	85.00	68.76	63.76
		Cr				
Cr^{3+}	0	0	0	0.02	0.15	0.26
CrO^+	0	0	0	87.73	70.35	60.12
$CrOH^{2+}$	0	0	0	10.59	29.02	39.3
$HCrO_2^0$	0	0	0	1.63	0.47	0.32
CrO_2^-	0	0	0	0.01	0	0
CrO_4^{2-}	0	95.88	99.13	0	0	0
$HCrO_4^-$	0	4.12	0.87	0	0	0
$CrHA^{2+}$	0	0	0	0.02	0.01	0
		Mn				
Mn^{2+}	96.83	98.49	83.8	92.23	87.51	91.92
$MnOH^+$	0.06	0.04	0.08	0.01		
$MnCl^+$	0.01	0.01	0.06	0.59	1.16	3.48
$MnSO_4^0$	0.20	0.22	0.95	3.51	10.06	4.53
Mn HCO_3^+	1.01	0.68	2.2	3.66	1.27	0.07
MnO_4-	1.87	0.54	12.9	0	0	0
MnO_4--		0	0.01	0	0	0
$MnHA^+$	0.02	0.02	0	0	0	0
		Fe				
Fe^{2+}	0	0	0	14.11	62.3	86.98
$FeOH^+$	0	0	0	0.03	0.05	0.04
$FeCl^+$	0	0	0	0.14	1.23	4.75
$FeSO_4^0$	0	0	0	0.95	12.66	7.63
$FeCO_3^0$	0	0	0	1.92	1.05	0.06
$Fe(OH)_2$ FA^-	100	100	100	82.85	22.71	0.54
		Ni				
Ni^{2+}	99.96	99.96	99.92	99.86	99.74	99.27
$NiOH^+$	0.04	0.04	0.07	0.01		
$NiCl^+$	0	0	0.01	0.13	0.26	0.73
$NiHA^+$	0	0	0	0	0	0
		Cu				
$HAsO_4^{2-}$	94.87	92.22	98.16	0	0	0
$H_2AsO_4^-$	5.11	7.77	1.78	0	0	0
$HAsO_2^0$	0	0	0	98.92	99.55	99.62
AsO_2^-	0	0	0	1.08	0.45	0.38
		Sr				
Sr^{2+}	98.19	98.44	92.86	83.30	66.76	81.37
$SrCl^+$	0.01	0.01	0.07	0.55	0.87	2.8
$SrCl_2^0$	0	0	0	0	0.01	0.15
$SrSO_4^0$	0.90	0.97	4.71	13.71	31.68	15.64
$SrCO_3^0$	0.11	0.05	0.59	0.09	0.01	0
$SrHCO_3^+$	0.79	0.53	1.77	2.35	0.67	0.04
		Mo				
MoO_4^{2-}	99.98	99.97	99.99	99.96	99.92	99.92
$HMoO_4^-$	0.02	0.03	0.01	0.04	0.08	0.08
		Cd				
Cd^{2+}	97.36	97.49	83.85	35.39	19.95	5.7
$CdOH^+$	0.24	0.16	0.32	0.01		
$CdCl^+$	2.10	2.15	15.02	57.58	62.44	46.01
$CdCl_2^0$	0	0	0.15	6.42	16.15	36.38
$CdCl_3^-$	0	0	0	0.19	1.33	10.39
$CdCl_4^{2-}$	0	0	0	0	0.05	1.52
$CdHCO_3^+$	0.30	0.2	0.66	0.41	0.08	0
		Pb				
Pb^{2+}	1.03	1.74	0.25	1.87	9.59	16.25
$PbOH^+$	64.95	73	40.07	26.53	36.86	34.8
PbO^0	0.01	0.01	0.01			
$PbCl^+$	0.01	0.01	0.01	0.64	6.27	27.01
$PbCl_2^0$	0	0	0	0.04	0.99	13.39
$PbCl_3^-$	0	0	0	0	0.04	1.88
$PbCl_4^{2-}$	0	0	0	0	0	0.78
$PbHS^+$	0	0	0	0.01	0.02	0.01
$PbSO_4^0$	0.01	0.02	0.02	0.36	5.18	3.44
$PbCO_3^0$	33.84	24.97	59.64	70.52	41.02	2.44
$PbHCO_3^+$	0	0	0	0.01	0.03	0
$PbHA_2^0$	0	0	0	0	0	0
$PbHA^+$	0.15	0.25	0	0.02	0	0
		U				
UO_2OH^+	0.02	0.06	0	99.99	99.96	100
$UO_2CO_3^0$	1.84	5.11	11.52	0	0	0
UO_2	55.66	57.18	0	0	0	0

							$(CO_3)_2^{2-}$						
Cu^+	0	0	0	0.19	0.02	0	$UO_2(CO_3)_3^{4-}$	26.98	12.16	88.19	0	0.01	0
$CuOH^0$	0	0	0	0.04	0	0	UO_3^0	14.32	24.48	0.20	0.01	0.03	0
$CuCl^0$	0	0	0	1.31	0.34	0.04	HUO_4^-	1.18	1.01	0.04	0	0	0

3.1.1. Fulvic Aqueous Species

Fulvic acids (FA^{2-}) are fully bound to Fe in the $Fe(OH)_2FA^-$ complex in all types of natural surface and groundwater ZS, ZW, DB, L1, L2 and Vmz (Figure 2a).

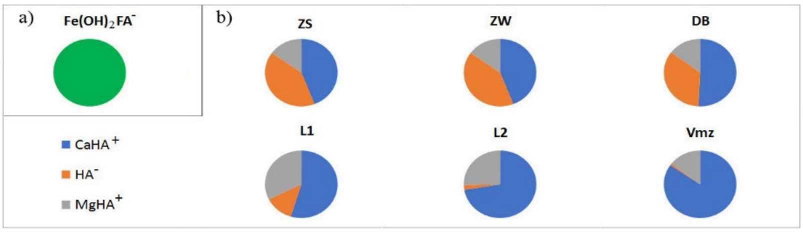

Figure 2. Main aqueous species of a) fulvic acids and b) humic acids in natural waters of the study area (%).

Fe has a high affinity for organic matter and ranks first among competitive complex formation in all landscape-climatic zones [42]. Accordingly, when calculating, it is complexed with FA^{2-} in the first place, taking from the balance of the FA entered into the model everything that can be pulled onto itself. The FA^{2-} remaining in the solution is generally distributed over other metals, but in our case this is not observed, due to the rather high content of Fe.

The high content of iron in fresh oxygen waters with positive values of the redox potential is due to the oxidation of $Fe^{2+} \rightarrow Fe^{3+} + e$ and the subsequent formation of stable complex compounds of Fe^{3+} with FA^{2-}. In our case, the hydroxofulvate complex $Fe(OH)_2FA^-$ turned out to be the most competitive. Organo-mineral complexes of Fe are very stable. The formation of these complexes does not allow the precipitation of Fe in the form of hydroxide [43]. According to calculations, after the FA specified in the balance is exhausted, Fe precipitates in the form of goethite. That is, for correct calculations of the amount of precipitated Fe minerals, it is critical to correctly determine the amount of organic matter in natural waters. In fresh waters ZS, ZW and DB iron concentrations adjusted for deposition (see Tables 2 and 4) are 315, 180 and 33.84 μg/kg H_2O, respectively, and are limited by FA^{2-} concentrations of 28.2, 16.1 and 3.03 mg/kg H_2O (see Table 2), based on the ratio FA/Fe = 5000/55.84. In brackish and saline waters L1, L2 and Vmz, FA^{2-} concentrations are 7.55, 2.92 and 2.56 mg/kg H_2O (see Table 2), and they allow Fe^{3+} to be present in organo-mineral complexes in amounts of 84.3, 32.6 and 28.6 μg/kg H_2O, respectively. In this case, the total iron content, taking into account deposition (see Tables 2 and 4), in brackish and saline waters L1, L2 and Vmz are 91, 142 and 5314 μg/kg H_2O.

Table 4. Simulation results of sedimentation from the surface waters of the Zolotitsa River and groundwater in the initial natural conditions.

	ZS	ZW	DB	L1	L2	Vmz
Minerals, mol/kg H_2O						
Ankerite $CaFe(CO_3)_2$	0	0	0	2.22E-05	3.09E-05	0
Chalcocite Cu_2S	0	0	0	9.44E-09	1.45E-08	2.27E-09
Chromite $FeCr_2O_4$	**0**	**0**	**0**	9.52E-09	1.48E-08	1.78E-07
Dolomite $CaMg(CO_3)_2$	0	0	0.000196	1.75E-04	0	0
Gibbsite $Al(OH)_3$	2.11E-06	2.11E-06	2.42E-07	9.31E-07	1.26E-06	6.93E-06
Goethite $FeO(OH)$	4.29E-07	2.85E-06	2.25E-08	0	0	0
Pyrolusite MnO_2	2.44E-07	2.44E-07	2.28E-07	0	0	0
Siderite $FeCO_3$	0	0	0	0	0	2.22E-05
Sphalerite ZnS	0	0	0	1.75E-07	5.86E-08	8.26E-08
UO_2(cr)	**0**	**0**	**0**	6.16E-09	6.34E-08	1.97E-10
Galena PbS	0	0	0	5.20E-09	0	0
(Ca,Sr,Zn,Pb,Mn)CO_3, mol/kg H_2O (solid solution)						
Ca	0	0	6.01E-06	5.42E-06	3.21E-04	0
Sr	0	0	1.65E-06	4.13E-06	1.17E-04	0
Zn	**0**	**0**	6.67E-09	4.41E-09	1.03E-07	**0**
Pb	0	0	1.87E-10	1.71E-09	9.71E-09	0
Mn	0	0	8.18E-17	2.75E-07	8.29E-06	0

In general, the distribution of aqueous species of Fe in natural waters of the study area depends on the redox conditions in the aquifer and their FA content. In anoxic groundwater of the Mezen Formation, Vmz, at a depth of more than 200 m, Fe^{2+} (86.98%) and inorganic complexes $FeSO_4^0$ and $FeCl^+$ predominate (Figure 3). The content of $FeCO_3^0$ and $FeOH^+$ is relatively low, 0.06 and 0.04%, respectively.

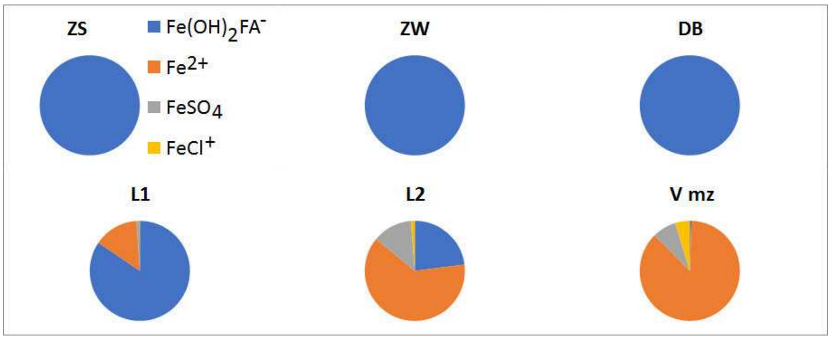

Figure 3. Main migratory species of Fe in natural waters of the study area (%).

Groundwater, pumped from the "lens" in the Vendian Padun Formation, which is localized near the Lomonosovskaya pipe (L2), is also dominated by Fe^{2+} (62.3%), but there is already an organomineral complex (22.71%), $FeSO_4^0$ (12.66%) , $FeCl^+$ (1.23%), $FeCO_3^0$ (1.05%) and $FeOH^+$ (0.05%). Groundwater, pumped from the "lens" in the Vendian Padun Formation, which is localized near the Karpinskaya pipe (L1), contains more organic matter and is dominated by the fulvate complex $Fe(OH)_2FA^-$ (82.85%). The content of Fe^{2+} is 14.11%, $FeCO_3^0$ 1.92%, $FeSO_4^0$ 0.95%, $FeCl^+$ 014% and $FeOH^+$ 0.03%. In oxidizing groundwater, pumped from dewatering boreholes in the Vendian Padun Formation (DB) and in the surface waters of the Zolotitsa River (ZS and ZW), all dissolved iron binds to the fulvate complex.

doi:10.20944/preprints202305.0238.v1

3.1.2. Humic Aqueous Species

With Humic acids, such a sharp competitive complex formation does not occur as with fulvic acid. It is distributed more evenly among different elements. The proportion of HA^- is highest in the $CaHA^+$ form, rising from 43.94% in Z to 84.37% in Vmz (Figure 2b). In the same direction, both the calcium concentration and the TDS value in the water increase. The proportion of HA^- and in the form of $MgHA^+$ is significant, 15.02-32.27%. In addition, $ZnHA^+$ is present in river water at 0.33%, decreasing to 0.05-0.02% in DB, L1 and L2 and completely absent in Vmz. $MnHA^+$ is seen in Vmz (0.22%) decreasing to 0.12-0.08% in L1 and L2. $CuHA^+$ is 0.01% in Z, 0.02 in Vmz. $SrHA^+$ is also found in Z, L1 and L2 (0.01) as well as in Vmz (0.04%). The content of HHA^0 does not exceed 0.01%. At the same time, HA^- in the dissociated form is also widely represented in the surface waters of the Zolotitsa River, its content is 40.67% (Figure 2b). In DB, L1, L2 and Vmz, its content consistently decreases from 34.49 to 0.86%, "balancing" the increasing $CaHA^+$ values (Figure 4).

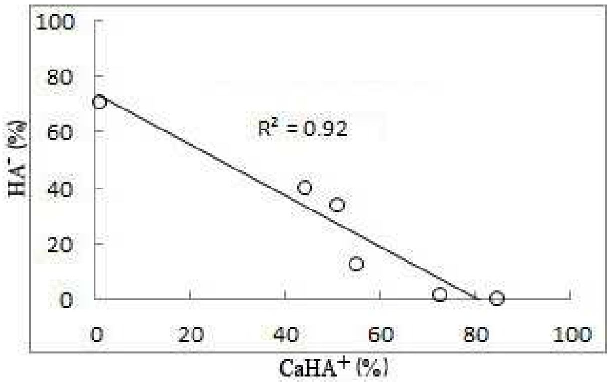

Figure 4. Relationship between HA^- and $CaHA^+$ (%) in natural waters of the study area.

In the distribution structure of aqueous species of the chemical elements-macrocomponents in natural waters of the study area, organo-mineral complexes play a less prominent role. Thus, the proportion of $CaHA^+$ in the Ca migratory species is only 0.01% in Z, while the proportion of $MgHA^+$ in the Mg migratory species is generally lower than 0.01% in all types of waters. In the aqueous species of the trace elements, the participation of HA^+ is somewhat higher. The share of $ZnHA^+$ in Zn migratory species is 0.16-0.19% in ZS-ZW and 0.01% in DB and L1. For $CuHA^+$, the corresponding distribution is expressed as 0.14-0.31% in ZS-ZW, for $PbHA^+$ as 0.15-0.25% in ZS-ZW and 0.02% in L1, for $MnHA^+$ as 0.02% in ZS and ZW. It can be noted that the proportion of organo-mineral complexes with Zn, Cu and Pb in river water is higher in winter than in summer.

In general, for natural surface waters of the taiga zone with sufficient alkalinity, Moiseenko et al. [42] obtained the following regularity in the predominant distribution of metals in bonding into organic complexes: Fe > Al > Pb > Co > Ni > Zn > Cd > Cu > Mg > Ca > Cr > Mn > Sr. In our case, it looks somewhat different: Fe > Zn > Cu > Pb > Mn > Ca > Mg > Sr, probably due to the local specificity of the studied watercourse.

3.1.3. Inorganic Species

Elements related to the macrocomponent composition of waters - calcium, magnesium, sodium and potassium, migrate mainly in ion-dissolved form. The greatest contribution to complex formation with calcium and magnesium in fresh waters is made by hydrocarbonate, sulfate and carbonate complexes, however, the vast majority of both elements (94-99%) are in the form of uncomplexed ions. In brackish and saline waters, the proportion of the latter is somewhat reduced (72-90%) due to an increase in the role of sulfate complexes (Table 3). Sodium and potassium in the groundwater of the territory are also mainly in the form of free ions (more than 99% on average) [44].

Manganese in compounds exhibits oxidation states from +2 to +7, due to the specifics of the electronic configuration of the valence layer of atoms. It, like iron, belongs to the number of elements whose oxidized forms are much less soluble than the reduced ones. However, in contrast to iron, oxidation of $Mn^{2+} \rightarrow Mn^{3+}$ and subsequent hydrolysis of $Mn^{3+} + 3OH^-$ with precipitation of Mn(OH) require much higher values of the redox potential (Eh > +600 mV) than those observed in the natural waters of the study area (Eh < + 281 mV). In addition, unlike iron, it also has a weak ability to complex (see section 3.1.2) and therefore migrates mainly in the form of Mn^{2+} (84-98%). The second dominant form of manganese occurrence in fresh waters is its carbonate complex $MnHCO_3^+$ (0.7-2.2%), while $MnSO_4$ (4-10%) dominates in brackish and saline waters. At the same time, according to calculations, Mn is deposited from surface waters in the amount of 13.4 μg/kg H_2O as part of pyrolusite, and from 12 to 455 μg/kg H_2O co-precipitates with calcite in groundwater DB, L1 and L2.

Aluminum under natural pH conditions is characterized by the main forms of migration AlO_2^- (63.76–97.7%) and AlOOH (2.29–32.13%). It is deposited in the composition of gibbsite from surface waters in the amount of 63.3 μg/kg H_2O. From groundwater, the deposition rate increases from 7.26 to 208 μg/kg H_2O with TDS increasing from 0.45 to 21.7 g/kg H_2O.

The calculations performed show a high degree of copper complexation, the dominant form of which in fresh waters is $CuCO_3^0$ (74.63-91.31%). In relatively small amounts, copper is present in the form of CuO^0 (7.34–12.86%) and $CuOH^+$ (0.55–2.82%), as well as in the ionic form Cu^{2+} (0.77–10.17%). In brackish and saline waters, the main forms of copper migration are $CuCl^{2-}$ (24.38-80.86%) and $CuCl_3^{2-}$ (17.6-75.58%).

Zinc forms a significant amount of complexes; the free ionic form Zn^{2+} accounts for 44.46–83.25%. The carbonate complex $ZnCO_3^0$ (0.06–37.52%), the hydroxo complex $ZnOH^+$ (0.65–19.02%), and the sulfate complex $ZnSO_4^0$ (0.41–23.06%) dominate. Small amounts of zinc (0.44-11.7 μg/kg H_2O) precipitate from groundwater as sphalerite and $CaCO_3$.

In surface and groundwater, strontium is a geochemical analogue of calcium and, like calcium, is a weak complexing agent. The main forms of strontium: Sr^{2+} (66.76-98.44%), $SrSO_4^0$ (0.9-31.68%), $SrHCO_3^+$ (0.04-2.35%). It co-precipitates with calcite from groundwater in significant amounts from 0.14 to 10.3 mg/kg H_2O.

The behavior of uranium in water depends on redox and acid-base conditions. In surface waters, it is in the oxidized form 6+ and migrates as part of the uranyl-carbonate complexes $UO_2(CO_3)_2^{2-}$ (55.66-57.18%) and $UO_2(CO_3)_3^{4-}$ (26.98-12.16%), as well as in the form UO_3^0 (14.32-24.48%), the ratio of which is determined by acid-base conditions. In fresh groundwater of DB, it is also under oxidizing conditions, but the increased alkalinity of water determines a slightly different ratio of carbonate complexes: $UO_2(CO_3)_3^{4-}$ (88.19%) and $UO_2(CO_3)^0$ (11.52%). Finally, in the reducing environment of groundwater L1, L2 and Vmz, it almost completely precipitates, and the uranium remaining in solution migrates in the form of UO_2OH^+.

Nickel and cadmium migrate predominantly in the ionic form. Molybdenum predominates in the form of MoO_4^{2-}; for chromium, the CrO_4^{2-} form is characteristic in fresh waters; in salty waters, it is in the form of CrO^+. Arsenic migrates in fresh waters as part of $HAsO_4^{2-}$, in saline waters - $HAsO_2^0$; lead, respectively, $PbOH^+$ and $PbCO_3^0$.

3.2. Estimated Aqueous Organic and Inorganic Species in the Zolotitsa River when Draining Groundwater is Discharged into it from a System of Drainage Wells

3.2.1. Fulvic and Humic Species

Simulation results of changes in composition of dominant migration species of chemical elements in Zolotitsa River with discharged drainage groundwater from a system of dewatering boreholes показаны в таблице 5.

Table 5. Simulation results of changes in composition of dominant migration forms of chemical elements in Zolotitsa River with discharged drainage groundwater from a system of dewatering boreholes.

Aqueous species	Scenarios of mixing of river waters with drainage groundwater											
	1S	1W	2S	2W	3S	3W	4S	4W	5S	5W	6S	6W
% of total content												
FA												
Fe(OH)$_2$FA$^-$	100	100	100	100	100	100	100	100	100	100	100	100
HA												
HA$^-$	33.03	30.96	32.82	30.93	8.27	8.20	23.58	22.19	12.42	12.07	8.6	8.47
CaHA$^+$	49.14	50.57	42.43	44.93	65.67	68.55	60.92	62.38	71.5	73.02	74.75	76.2
MgHA$^+$	17.74	18.38	24.61	24.00	26.01	23.21	15.46	15.38	16.06	14.89	16.64	15.32
SrHA$^+$	0.01	0.01	0.01	0.01	0.01	0.01	0	0	0	0	0	0
ZnHA$^+$	0.08	0.08	0.13	0.13	0.04	0.04	0.04	0.05	0.02	0.02	0.01	0.01
Al												
AlO$^+$	0	0.01	0.01	0.01	0.03	0.04	0.01	0.01	0.01	0.02	0.02	0.03
AlOOH	2.22	2.54	2.26	2.56	4.7	5.06	2.64	2.97	3.64	3.98	4.35	4.71
AlO$_2^-$	97.78	97.45	97.73	97.43	95.27	94.90	97.35	97.02	96.35	96	95.63	95.26
As												
AsO$_4^{3-}$	0.06	0.06	0.07	0.06	0.04	0.04	0.06	0.05	0.05	0.04	0.04	0.04
HAsO$_4^{2-}$	97.99	97.90	98.07	98.01	96.47	96.52	97.7	97.65	97.03	97.04	96.63	96.65
H2AsO$_4^-$	1.95	2.04	1.86	1.93	3.49	3.44	2.24	2.3	2.92	2.92	3.33	3.31
Ca												
Ca^{2+}	94.88	95.02	93.67	93.75	88.4	88.42	95.17	95.19	95.01	94.96	94.6	94.57
CaCl$^+$	0.05	0.05	0.17	0.16	0.33	0.32	0.11	0.11	0.26	0.25	0.38	0.37
CaSO$_4^0$	1.49	1.46	3.18	3.12	10.5	10.40	2.14	2.1	3.34	3.3	4.03	3.98
CaCO$_3^0$	1.86	1.57	1.49	1.29	0.23	0.22	1.21	1.06	0.52	0.48	0.32	0.3
CaHCO$_3^+$	1.72	1.90	1.49	1.67	0.54	0.64	1.37	1.54	0.87	1.01	0.67	0.78
Cd												
Cd^{2+}	88.3	87.70	69.08	67.42	51.92	49.73	77.63	76.34	59.45	57.41	49.66	47.52
CdOH$^+$	0.49	0.32	0.33	0.22	0.09	0.06	0.34	0.22	0.16	0.11	0.1	0.07
CdCl$^+$	10.53	11.28	29.45	31.09	45.3	47.13	21.27	22.62	38.67	40.52	47.28	49.02
CdCl$_2^0$	0,07	0.08	0.72	0.84	2.54	2.91	0.33	0.38	1.5	1.73	2.79	3.2
CdCl$_3^-$	0	0	0	0.01	0.03	0.05	0	0	0.01	0.02	0.04	0.05
CdHCO$_3^+$	0.62	0.62	0.42	0.42	0.12	0.12	0.43	0.44	0.21	0.21	0.13	0.14
Cr												
CrO$_4^{2-}$	99	99	9905	99.05	98.21	98.31	98.85	98.87	98.5	98.56	98.29	98.37
HCrO$_4^-$	1	1	0.95	0.95	1.79	1.69	1.15	1.13	1.5	1.44	1.71	1.63
Cu												
Cu^{2+}	0.92	0.94	1.12	1.13	6.42	5.87	1.4	1.39	3.21	3.01	5.06	4.68
CuOH$^+$	0.87	0.64	0.94	0.68	2.06	1.43	1.06	0.76	1.54	1.08	1.88	1.31

CuO^0	13.57	7.76	13.52	7.74	12.47	7.22	13.5	7.74	13.12	7.56	12.78	7.38
$CuCl^+$	0	0	0.01	0.01	0.13	0.13	0.01	0.01	0.05	0.05	0.11	0.11
$CuSO_4^0$	0.02	0.02	0.06	0.05	1.16	1	0.05	0.04	0.17	0.15	0.33	0.29
$CuCO_3^0$	84.6	90.62	84.33	90.37	77.73	84.32	83.96	90.04	81.88	88.12	79.81	86.2
$CuHCO_3^+$	0.01	0.01	0.01	0.01	0.02	0.02	0.01	0.01	0.02	0.02	0.02	0.02
$CuHA^+$	0.01	0	0.01	0.01	0.01	0.01	0.01	0.01	0.01	0.01	0.01	0.01
$CuHA_2^0$	0	0.01	0	0	0	0	0	0	0	0	0	0
Fe												
$Fe(OH)_2$	100	100	100	100	100	100	100	100	100	100	100	100
FA^-												
Mg												
Mg^{2+}	94.93	95	92.54	92.69	82.93	83.44	94.53	94.58	93.23	93.38	92.23	92.41
$MgOH^+$	0.01	0.01	0.01	0.01	0	0	0.01	0.01	0.01	0	0	0
$MgCl^+$	0.08	0.08	0.28	0.28	0.53	0.55	0.18	0.18	0.43	0.44	0.63	0.65
$MgCl_2^0$	0	0	0	0	0.02	0.02	0	0	0.01	0.01	0.02	0.02
$MgSO_4^0$	2.32	2.19	4.94	4.68	15.89	15.26	3.32	3.15	5.2	4.93	6.29	5.99
$MgCO_3^0$	0.98	0.87	0.78	0.71	0.12	0.12	0.63	0.58	0.27	0.26	0.17	0.17
$MgHCO_3^+$	1.68	1.85	1.45	1.62	0.51	0.61	1.33	1.5	0.85	0.98	0.65	0.76
Mn												
Mn^{2+}	76.48	86.59	79.28	87.52	91.11	91.98	84.54	90.65	92.47	94.49	94.14	95.25
$MnOH^+$	0.11	0.08	0.1	0.07	0.04	0.03	0.09	0.07	0.07	0.04	0.05	0.03
$MnCl^+$	0.04	0.04	0.16	0.16	0.38	0.34	0.11	0.1	0.28	0.26	0.42	0.38
$MnSO_4^0$	0.69	0.74	1.55	1.63	6.24	6.04	1.09	1.12	1.88	1.83	2.32	2.23
$MnHCO_3^+$	1.82	2.06	1.65	1.85	0.73	0.79	1.6	1.76	1.11	1.2	0.87	0.94
MnO_4^-	20.83	10.48	17.23	8.76	1.5	0.82	12.56	6.3	4.19	2.18	2.19	1.17
MnO_4^{2-}	0.02	0.1	0.02	0.01	0	0	0.01	0	0	0	0	0
$MnHA^+$	0.01	0	0.01	0	0	0	0	0	0	0	0	0
Mo												
MoO_4^{2-}	99.99	99.99	99.99	99.99	99.99	99.99	99.99	99.99	99.99	99.99	99.99	99.99
$HMoO_4^-$	0.01	0.01	0.01	0.01	0.01	0.01	0.01	0.01	0.01	0.01	0.01	0.01
Ni												
Ni^{2+}	99.89	99.92	99.87	99.9	99.89	99.91	99.9	99.93	99.89	99.91	99.88	99.89
$NiOH^+$	0.1	0.07	0.09	0.06	0.03	0.02	0.08	0.05	0.05	0.04	0.04	0.03
$NiCl^+$	0.01	0.01	0.04	0.04	0.08	0.07	0.02	0.02	0.06	0.05	0.08	0.08
Pb												
Pb^{2+}	0.31	0.30	0.37	0.35	1.41	1.25	0.43	0.4	0.82	0.74	1.17	1.05
$PbOH^+$	44.18	42.78	46.05	44.36	65.71	63.21	49.15	47.2	58.72	56.2	63.5	60.99
PbO^0	0.02	0.01	0.02	0.01	0.01	0.01	0.02	0.01	0.02	0.01	0.02	0.01
$PbCl^+$	0.01	0.01	0.04	0.03	0.28	0.25	0.03	0.03	0.12	0.11	0.26	0.23
$PbCl_2^0$	0	0	0	0	0.01	0.01	0	0	0	0	0.01	0
$PbSO_4^0$	0.01	0.01	0.04	0.03	0.49	0.42	0.03	0.03	0.09	0.07	0.15	0.13

$PbCO_3^0$	55.46	56.88	53.47	55.20	32.08	34.84	50.32	52.2	40.22	42.86	34.88	37.58
$PbHA^+$	0.01	0.01	0.01	0.00	0.01	0.01	0.01	0.01	0.01	0.01	0.01	0.01
Sr												
Sr^{2+}	93.88	94.21	90.19	90.60	76.53	77.09	92.84	93.19	90.69	90.99	3.62	89.66
$SrCl^+$	0.05	0.05	0.17	0.17	0.3	0.30	0.12	0.11	0.27	0.26	0.02	0.38
$SrSO_4^0$	3.75	3.59	7.74	7.44	22,5	22.07	5.31	5.06	8.05	7.77	89.56	9.23
$SrCO_3^0$	0.6	0.50	0.46	0.39	0.06	0.06	0.38	0.33	0.16	0.14	0.9	0.09
$SrHCO_3^+$	1.72	1.65	1.44	1.40	0.46	0.48	1.35	1.31	0.83	0.84	5.9	0.64
U												
UO_2OH+	0	0	0	0	0.01	0	0	0	0	0	0.01	0
$UO_2CO_3^0$	0.09	0.07	0.07	0.05	0.56	0.39	0.14	0.11	0.34	0.24	0.50	0.35
$UO_2(CO_3)_2^{2-}$	18.9	15.32	15.02	12.03	29.96	23.95	21.0	17.3	28.1	22.42	30.27	24.9
$UO_2(CO_3)_3^{4-}$	80.38	84.18	84.26	87.60	64.65	73.47	76.75	81.51	68.70	75.96	64.92	73.17
UO_3^0	0.69	0.36	0.54	0.27	4.40	2.01	1.11	0,56	2.62	1.24	3.89	1.82
HUO_4^-	0.15	0.07	0.11	0.05	0.42	0.18	0.20	0.09	0.33	0.14	0.41	0.17
Zn												
Zn^{2+}	42.01	48.14	45.5	51.33	66.6	70.64	49.88	55.76	63.37	68.71	69.36	74.09
$ZnOH^+$	25.76	16.72	24.49	15.84	13.76	8.83	24.26	15.71	19.67	12.62	16.59	10.64
ZnO^0	0.23	0.11	0.2	0.10	0.05	0.02	0.17	0.09	0.09	0.05	0.06	0.03
$HZnO_2^-$	0.01	0	0.01	0	0	0	0	0	0	0	0	0
$ZnCl^+$	0.03	0.03	0.12	0.10	0.35	0.28	0.08	0.07	0.25	0.2	0.4	0.32
$ZnCl_2^0$	0	0	0	0	0.01	0.01	0	0	0	0	0.01	0.01
$ZnSO_4^0$	1.06	1.13	2.48	2.60	12.67	12.66	1.79	1.88	3.58	3.62	4.73	4.76
$ZnCO_3^0$	30.46	33.37	26.78	29.58	6.33	7.30	23.42	26.02	12.72	14.43	8.58	9.84
$ZnHCO_3^+$	0.41	0.48	0.39	0.45	0.22	0.25	0.38	0.45	0.31	0.36	0.26	0.3
$ZnHA^+$	0.03	0.02	0.03	0.00	0.01	0.01	0.02	0.02	0.01	0.01	0.01	0.01

In mixing solutions, fulvic acids, as in natural waters (Figure 2a), are completely bound to Fe in the $Fe(OH)_2FA^-$ complex in all 6 mixing scenarios. The formation of organo-mineral complexes of Fe is a classic scenario for the accumulation of Fe in natural waters.

Humic acids, as in natural waters, are distributed more evenly over different elements. The proportion of HA^- is maximal in the form of $CaHA^+$, rising from 42.43 in 2S to 76.2% in 6W (Figure 5a) relative to the total HA content, which is significantly higher than in natural river waters (43.94%) (Figure 2b). The difference between summer and winter periods is insignificant (2 - 6%), and in winter the relative percentage of $CaHA^+$ is higher than in summer. This pattern is observed because we are considering the percentage of complexes relative to the total content of HA in the system. Since the total HA content in the river is lower in winter than in summer, most of it is complexed with metals.

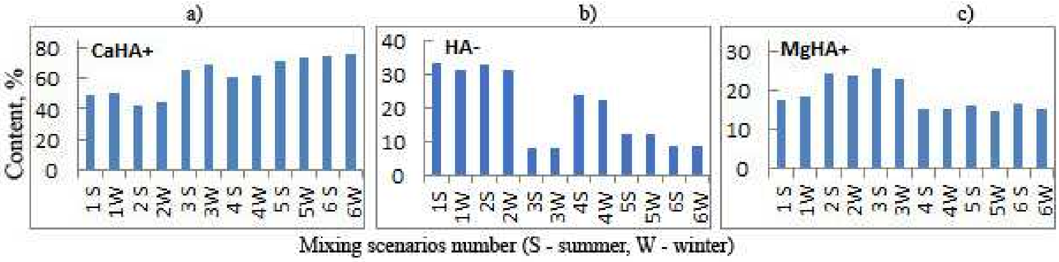

Figure 5. Main migratory species of humic acids in the Zolotitsa River when draining groundwater is discharged into it from a system of drainage wells (%).

The content of organo-mineral complexes in the form of $MgHA^+$ in the mixture of river waters with drainage waters (14.89-26.01%) (Figure 5c) is comparable to their content in natural river waters (15.02%). In addition, $ZnHA^+$ is present in mixing solutions according to scenarios 1 and 2 in an amount of 0.08-0.13%, decreasing to 0.04-0.01% according to scenarios 3-6, which is significantly lower than in natural river water (0.33). $SrHA^+$ is set in the amount of 0.01% only in mixing solutions according to scenarios 1-3. NA^- in free form in mixing solutions according to scenarios 1 and 2 is contained in the amount of 30.93-33.03%, according to scenarios 3-6 it decreases to 8.2-23.58% (Figure 5b), which is significantly lower than in the natural waters of the river (40.67). This is due to an increase in the concentrations of Ca, Mg, Zn, Sr in mixing solutions compared to their concentrations in river waters. In other words, in the mixing solution, metals are complexed, which mainly come from discharged groundwater, with organic matter, which is contained in river waters. The formed organo-mineral complexes are very stable and the metals complexed in them can migrate in this form over long distances.

The percentage of HA^- and $MgHA^+$ in mixing solutions is generally lower in winter than in summer; the contents of $ZnHA^+$ and $SrHA^+$ are basically the same in summer and winter.

In the distribution structure of aqueous species of the chemical elements-macrocomponents in mixed solutions, organo-mineral complexes play a less prominent role. Thus, the proportion of $CaHA^+$ in Ca aqueous species and the proportion of $MgHA^+$ in Mg migratory species are below 0.01% in all types of waters. In aqueous species of the trace elements, HA^+ participation is not much higher. The proportion of $ZnHA^+$ in Zn aqueous species is 0.01-0.03%, while in natural river waters it is in the range of 0.16-0.19%. For $CuHA^+$ and $PbHA^+$, the corresponding distribution is expressed as 0.01%, which is significantly lower than the distribution in natural river waters (0.14-0.31% and 0.15-0.25%, respectively). This is a consequence of the fact that the concentration of trace elements in mixing solutions is much higher than in river waters, while the content of organic matter, on the contrary, is lower. The proportion of $MnHA^+$ (0.01%) was established only in mixing solutions according to scenarios 1S and 2S and is close to the corresponding value in natural river waters (0.02%). At the same time, in mixing solutions, in general, the pattern noted in section 3.1.2 for natural river waters in the predominant distribution of metals in binding into organic complexes is preserved: Fe > Zn > Cu > Pb > Mn > Ca > Mg > Sr.

3.2.2. Inorganic Species

For elements related to the macrocomponent composition of waters, there is a decrease in the proportion of uncomplexed calcium and magnesium ions in mixing solutions (82.93-95.19%) compared to natural river waters (98.49-98.93%) mainly due to an increase in the role of sulfate complexes (1.46-15.89%) pulled up to the drainage system mainly from lens L2.

The proportion of uncomplexed manganese ions is also lower in mixed solutions (76.48–95.25%) compared to natural river waters (96.83–98.49%), mainly due to an increase in the proportion of MnO_4^- to 20.83% in summer and 10.48% in winter according to scenario 1 and to 17.23 % in summer and 8.76% in winter according to scenario 2 (Table 5).

The proportion of uncomplexed strontium ions is lower in mixed solutions (76.53–94.21%) compared to natural river waters (98.19–98.44%), mainly due to an increase in the proportion of $SrSO_4^0$ (3.59–22.66%) and $SrHCO3^+$ (0.46–5.9%) as compared with with the contents of these complexes in natural river waters (0.9–0.97% and 0.53–0.74%, respectively).

The content of aluminum in the form of AlO_2^- (94.9–97.78%) in mixed solutions is slightly higher than in natural river waters (93.04–94.48%) due to the reduction in the proportion of $AlOOH^0$ from 5.49–8.22% to 2.22–5.06%.

The content of copper in the form of $CuCO_3^0$ (77.73–90.62%) in mixed solutions is also higher than in natural river waters (74.63–80.19%) due to the reduction in the proportion of Cu^{2+} from 4.77–10.17% to 0.92–5.06% and CuO^0 from 11.97–12.86 % to 7.22-13.57%.

The free ionic form of Zn^{2+} accounts for 42.01–74.09% in mixed solutions, which is significantly lower than in natural river waters (70.7–80.12%). The most significant decreases are associated with an increase in the percentage content of $ZnCO_3^0$ (6.33–30.46%), $ZnOH^+$ (8.83–25.76%), $ZnSO_4^0$ (1.06–12.67%) compared with the contents of these complexes in natural river waters (4.61–9.33%, 14.32–19.02 and 0.41-0.49%, respectively).

The ratio of uranium carbonate complexes in mixing solutions has changed due to the involvement of groundwater. The content of $UO_2(CO_3)_3^{4-}$ increased to 64.92-87.6%, and the content of $UO_2(CO_3)_2^{2-}$ decreased to 12.03-30.27% compared with natural river waters, in which the content of $UO_2(CO_3)_3^{4-}$ is 12.16-26.98%, and the content of $UO_2(CO_3)_2^{2-}$ is 55.66-57.18%.

Nickel migrates predominantly in the ionic form in mixing solutions. The percentage of Cd^{2+} decreased due to the attraction of $CdCl^+$ from groundwater. Molybdenum still predominates in the form of MoO_4^{2-}; the same shape is characteristic of chromium. Arsenic still migrates mainly as $HAsO_4^{2-}$; lead, respectively, is characterized by $PbOH^+$ and $PbCO_3$ complexes.

3.3. Influence of DOC on the Intensity of Precipitation of Chemical Elements from Mixing Solutions

According to the simulation results, the concentration of Fe in solution in summer is higher than in winter: 82-91 μg/kg H_2O in winter and 127-136 μg/kg H_2O in summer (Figure 6a, Table 6). This is explained by the fact that Fe in solution is in the form of $Fe(OH)_2FA^-$, that is, 1 mmol/kg H_2O of Fe^{3+} accounts for 1 mmol/kg H_2O of FA^-, and FA^- in solution is higher in summer and less in winter (Table 6). Due to the strong affinity of Fe with organic matter, the entire amount of fulvic acid specified in the balance of the model is consumed for the formation of Fe organo-mineral complexes that retain Fe in solution. The free iron remaining in the mixing solutions precipitates in the form of Goethite FeO(OH) (Table 7). Naturally, more Fe is deposited in winter than in summer (Figure 6b). Figure 6b also shows the amount of precipitating Fe calculated assuming no DOC in the mixing solutions. In this case, when about 5000 m^3/h of drainage water is discharged into the river, the mass of precipitating iron according to scenario 3 can reach 28.9 t/y. When DOC is taken into account, this mass will decrease to 21 t/y in summer and to 23.6 t/y in winter, that is, it will be 27 and 18% less, respectively. According to the most favorable scenario 1, which will be realized during the longest periods of the deposit operation, the mass of deposited iron will be 8.8 t/y without taking into account DOC. When DOC is taken into account, this mass will decrease to 0.58 t/y in summer and to 3.55 t/y in winter, that is, it will be 93 and 60% less, respectively.

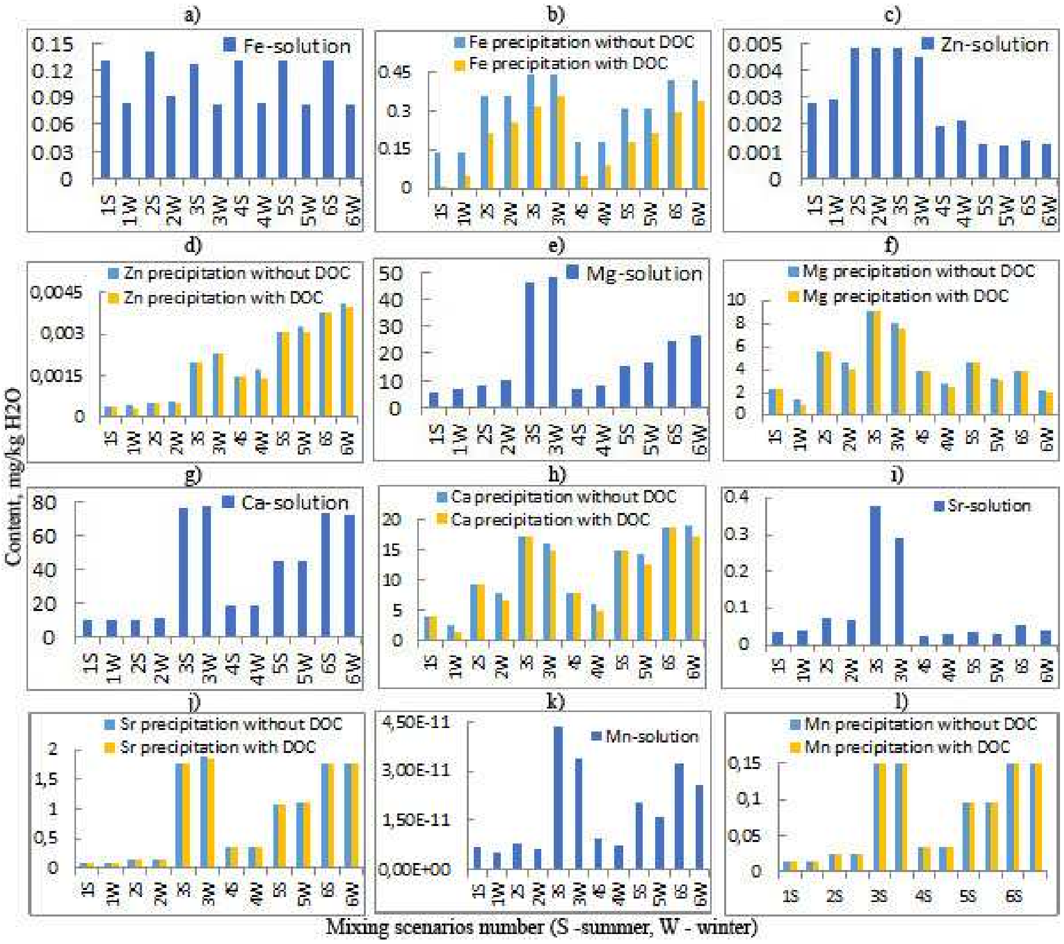

Figure 6. Comparison of the amount of deposited elements with and without DOC.

Table 6. Simulation results of changes in composition of water in Zolotitsa River with discharged drainage groundwater from a system of dewatering boreholes.

	Scenarios of mixing of river waters with drainage groundwater					
	1S	1W	2S	2W	3S	3W
			mg/kg H_2O	**H_2O**		
FA	11.4	7.4	12.2	815	11.4	7.35
HA	0.64	0.412	0.68	0.45	0.64	0.41
Na	72	72	187	187	382	382
Mg	5.25	6.76	8.34	9.97	46.4	47.9
S	7.95	7.95	22.3	22.3	135	135
Cl	51.4	51.4	207	207	532	532
K	3.09	3.09	3.53	3.53	7.98	7.98
Ca	9.74	10.2	9.58	10.3	76.2	76.6
HCO_3^-	133	142	131	142	63	72.1
SO_4^{2-}	23.9	23.9	66.9	66.9	405	405
TDS	310	318	625	635	1,525	1,532
			µg/kg H_2O			
Al	0.90	0.5	0.89	0.5	0.43	0.25
Cr	0.54	0.54	0.6	0.6	0.7	0.7

Mn	6.81E-09	5.38E-09	8.08E-09	6.37E-09	4.36E-08	3.4E-08
Fe	127	82.6	136	91	127	82.1
Ni	0.17	0.17	0.29	0.29	0.46	0.46
Cu	0.19	0.19	0.36	0.36	0.47	0.47
Zn	2.8	2.85	4.77	4.75	4.75	4.49
As	0.57	0.57	0.53	0.53	0.53	0.53
Sr	35.1	38.2	72.4	67.8	380	293
Mo	1.92	1.92	4.49	4.49	2.05	2.05
Cd	0.0039	0.0039	0.0098	0.0098	0.0098	0.0098
Pb	0.017	0.017	0.086	0.076	0.014	0.011
U	4.71	4.71	3.86	3.86	6.12	6.12

Continuation of Table 6.

	Scenarios of mixing of river waters with drainage groundwater					
	4S	4W	5S	5W	6S	6W
			mg/kg H_2O			
FA	11.4	7.4	11.4	7.35	11.4	7.35
HA	0.64	0.41	0.64	0.41	0.64	0.41
Na	107	107	207	207	301	301
Mg	6.78	8.26	15	16.6	24.3	26.2
S	13	13	27.6	27.6	41.4	41.4
Cl	125	125	338	338	539	539
K	3.41	3.41	4.34	4.34	5.2	5.2
Ca	17.8	18.5	44.5	44.9	72.5	72.1
HCO_3^-	112	121	80.8	90.4	68.6	76.7
SO_4^{2-}	39	39	82.8	82.8	124	124
TDS	423	431	785	791	1,147	1,152
			µg/kg H_2O			
Al	0.76	0.43	0.55	0.32	0.46	0.27
Cr	0.66	0.66	1	1	1.32	1.32
Mn	9.45E-09	7.64E-09	2.03E-08	1.62E-08	3.24E-08	2.56E-08
Fe	127	82.6	127	82.1	127	82.1
Ni	0.19	0.19	0.23	0.23	0.27	0.27
Cu	0.19	0.19	0.19	0.19	0.2	0.2
Zn	1.94	2.1	1.29	1.23	1.4	1.24
As	0.57	0.57	0.58	0.58	0.59	0.59
Sr	25.1	28.2	32.8	27.6	51.6	39.2
Mo	1.97	1.97	2.9	2.09	2.21	2.21
Cd	0.0041	0.0041	0.0046	0.0046	0.0052	0.0052
Pb	0.003	0.0032	0.00071	0.00057	0.00048	0.00036
U	4.67	4.67	4.55	4.55	4.43	4.43

Table 7. Simulation results of changes in composition of precipitation in Zolotitsa River with discharged drainage groundwater from a system of dewatering boreholes.

	Scenarios of mixing of river waters with drainage groundwater					
	1S	1W	2S	2W	3S	3W
	Phase, mol/kg H_2O					
Dolomite	9.74E-05	3.57E-05	2.35E-04	1.67E-04	3.80E-04	3.16E-04
Gibbsite	8.49E-07	8.63E-07	9.62E-07	9.76E-07	1.03E-06	1.04E-06
Goethite	1.58E-07	9.66E-07	3.90E-06	4.71E-06	5.64E-06	6.45E-06
Pyrolusite	2.33E-07	2.33E-07	4.34E-07	4.34E-07	2.66E-06	2.66E-06
	(Ca,Sr,Zn,Pb,Mn)CO_3, mol/kg H_2O (solid solution)					
Ca	3.19E-06	2.58E-06	2.32E-06	2.37E-06	4.86E-05	5.72E-05
Sr	1.12E-06	1.09E-06	1.65E-06	1.71E-06	2.03E-05	2.13E-05
Zn	5.46E-09	4.71E-09	7.54E-09	7.75E-09	3.07E-08	3.47E-08
Pb	2.33E-10	2.31E-10	1.05E-09	1.09E-09	1.83E-09	1.85E-09
Mn	5.65E-17	3,99E-17	5.21E-17	4.44E-17	9.01E-16	8.54E-16

Continuation of Table 7.

	Scenarios of mixing of river waters with drainage groundwater					
	4S	4W	5S	5W	6S	6W
	Phase, mol/kg H_2O					
Dolomite	1.63E-04	1.02E-04	1.96E-04	1.28E-04	1.64E-04	8.29E-05
Gibbsite	8.98E-07	9.09E-07	1.03E-06	1.04E-06	1.16E-06	1.16E-06
Goethite	9.30E-07	1.74E-06	3.16E-06	3.97E-06	5.26E-06	6.07E-06
Pyrolusite	6.10E-07	6.10E-07	1.70E-06	1.70E-06	2.73E-06	2.73E-06
	(Ca,Sr,Zn,Pb,Mn)CO_3, mol/kg H_2O (solid solution)					
Ca	3.06E-05	2.42E-05	1.81E-04	1.88E-04	3.09E-04	3.51E-04
Sr	2.34E-08	4.10E-06	1.24E-05	1.25E-05	2.01E-05	2.02E-05
Zn	4.13E-06	2.09E-08	4.70E-08	4.80E-08	5.83E-08	6.07E-08
Pb	3.01E-10	3.00E-10	3.14E-10	3.14E-10	3.16E-10	3.17E-10
Mn	4.54E-16	3.08E-16	2.53E-15	2.18E-15	4.30E-15	4.04E-15

It should be noted that the concentration of Fe in the solution in summer exceeds the maximum permissible concentrations (MPCs) for fishery rivers (100 µg/kg H_2O) established in Russia due to the increased concentrations of DOC in mixing solutions. At the same time, in winter, the Fe content is lower than the MPCs, due to the decrease in the DOC content in the water. However, under natural conditions, the water of the Zolotitsa River contains Fe in the amount of 339 µg/kg H_2O, that is, drainage waters contribute to a decrease in the concentration of this element, which in this case should have a positive effect on salmon spawning. The negative impact of drainage water is associated with increased concentrations of molybdenum in them 2.7-18.1 µg/kg H_2O (Table 2). As a result, under all scenarios, Mo concentrations exceed MPCs (1 µg/kg H_2O), varying from 1.92 to 4.49 µg/kg H_2O. Elevated concentrations of Mo in the abiotic components of the study area are associated with its transport from the Baltic (Fenno-Scandinavian) shield located to the west, where it is widely present in apatite-nepheline ores [18].

The removal of OH- from the solution proceeds similarly to the precipitation of Fe (Table 7). The concentration of OH-, which is in solution as part of the $Fe(OH)_2FA^-$ complex compound, is also proportional to the concentrations of FA^-.

The amount of precipitating zinc is two orders of magnitude lower than the amount of precipitating iron and one order of magnitude less than the amount of dissolved zinc (Figure 6c,d). The mass of Zn precipitating in the composition of the CaCO3 solid solution (Table 7) according to scenario 6 can reach 0.19 t/y and practically does not depend on the season, since the share of $ZnHA^+$ in the total balance of zinc compounds is negligible.

In contrast to Fe, the concentrations of Ca, Mg, and C in solution with DOC are somewhat higher in winter than in summer: 10.2–76.5, 6.76–47.9, and 14.2–28 mg/kg H_2O and 9.55–76.2, 5.25–46.4, and 12.4–26.1 mg/kg H_2O, respectively (Figure 6e,g, Table 6). At the same time, the summer concentrations of these elements in the solution with DOC are identical to the concentrations in the solution without DOC [25]. Accordingly, their precipitation is somewhat worse in winter than in summer. Ca precipitates in summer from 4 to 18.9 mg/kg H_2O, and in winter from 1.53 to 17.4 mg/kg H_2O; Mg precipitates in summer from 2.33 to 9.12 mg/kg H_2O, and in winter from 0.86 to 7.58 mg/kg H_2O; C precipitates in summer from 2.39 to 9.96 mg/kg H_2O, and in winter from 0.9 to 8.52 mg/kg H_2O. At the same time, in summer, the precipitation of these elements is the same both in the presence of DOC and in its absence (Figure 6f,h, Table 7).

Strontium in solution is higher in summer, and correspondingly more precipitated in winter (Figure 6i-j). Manganese is practically absent in the solution, its precipitation is practically independent of the season (Figure 6k-l).

4. Conclusions

On the example of a diamond deposit developed by deep quarries, a forecast was made of the impact of drainage water discharge on the change in the composition of river waters and bottom sediments, taking into account the pulling of salt water into the drainage system. To achieve the set task, the thermodynamic modeling method implemented in the HCh software package was chosen. Modeling was performed according to various scenarios, taking into account changes in the total dissolved solids of groundwater from 0.5 to 21.7 g/kg H_2O. Since the surface waters of the region contain high concentrations of organic matter, the model took into account the possibility of the formation of organo-mineral complexes of metals. The role of DOC in the migration of chemical elements and its influence on the precipitation of chemical elements from mixing solutions is given.

It has been established that fulvic acid completely binds to Fe in the $Fe(OH)_2FA^-$ complex in all types of natural waters and under all mixing scenarios. With humic acid, such a sharp competitive complex formation does not occur. It is distributed among the various elements more evenly. The distribution of Fe migration forms in natural waters depends on the content of FA^{2-} in them and on the redox conditions in the aquifer. The main forms in brackish and saline waters are Fe^{2+} and inorganic complexes $FeSO_4$ and $FeCl^+$. It has been determined that the mass of precipitating iron in the absence of DOC in mixing solutions can reach 28.9 tons per year. In the presence of DOC, this weight is reduced by 18-27%. According to the most favorable scenario, the mass of deposited iron, excluding DOC, will be 8.8 tons per year. When taking into account DOC, it will be less by 60-93%. The amount of precipitating zinc is two orders of magnitude lower than the amount of precipitating iron and one order of magnitude less than the amount of dissolved zinc. The mass of precipitated Zn can reach 0.19 tons per year and practically does not depend on the season, since the share of $ZnHA^+$ in the total balance of zinc compounds is negligible. Comparison of the data obtained in calculations with allowance for organic matter with data without it showed that fulvic and humic acids make a significant contribution to the distribution of metals between the aqueous phase and bottom sediments. A high DOC content in water helps to retain metals in the water, so calculations in such environments must be made taking DOC into account.

This study contributed to a better understanding of the behavior of heavy metals in surface waters and sediments under anthropogenic pressures in order to improve the sustainable management of water resources in the face of anthropogenic activities.

Author Contributions: Conceptualization, formal analysis, and writing—original draft preparation, A.I.M.; methodology and investigation, E.S.S. and E.V.C. All authors have read and agreed to the published version of the manuscript.

Funding: This work was supported by the Russian Ministry of Education and Science (project no. 122011300333-1). The publication was supported by the Russian Science Foundation and the Government of the Arkhangelsk Region (project No. 23-27-10004).

Conflicts of Interest: The authors declare no conflicts of interest. The founding sponsors had no role in the design of the study; in the collection, analyses, or interpretation of data; in the writing of the manuscript, and in the decision to publish the results.

References

1. Akimova, T.A.; Kuzmin, A.P.; Khaskin, V.V. Ecology. Nature - Man - Technique. Moscow: UNITY-DANA, **2001**. (in Russian)
2. Bondarev, L G. Technogenesis is a new factor in the development of the Earth's nature. Earth and Universe. **1996**, 1, 30-37. (in Russian)
3. Gao, P.; Shang, J.; Wu, J.; Mu, Z.; Suo, M.; Fan, J.; Zheng, Y.; Cheng, Y.; Wang, Y. Distribution, Risk Assessment, and Source Identification of Potentially Toxic Elements in the Sediments of the Upper Reaches of Zhanghe River, Haihe Basin. *Sustainability* **2022**, *14*, 15885. https://doi.org/10.3390/su142315885
4. Sidkina, E.S.; Soldatova, E.A.; Cherkasova, E.V.; Konyshev, A.A.; Vorobey, S.S.; Mironenko, M.V. Fate of Heavy Metals in the Surface Water-Dump Rock System of the Mine Lupikko I (Karelia): Field Observations and Geochemical Modeling. *Water* **2022**, *14*, 3382. https://doi.org/10.3390/w14213382
5. Khomenko, M.; Kononenko, I.; Myronova, E. Ecological and technological aspects of iron-ore underground mining. *Mining of Mineral Deposits* **2017**, *11(2)*, 59-67. DOI:10.15407/MINING11.02.059
6. Samal, P.; Mohanty, A.K.; Khaoash, S.; Mishra, P. Hydrogeochemical Evaluation, Groundwater Quality Appraisal, and Potential Health Risk Assessment in a Coal Mining Region of Eastern India. *Water Air Soil Pollution* **2022**, *233*, 324. https://doi.org/10.1007/s11270-022-05811-6
7. Krodkiewska, M.; Spyra, A.; Cieplok, A. Assessment of pollution, and ecological status in rivers located in the Vistula and Oder river basins impacted by the mining industry in Central Europe (Poland). *Ecological Indicators* **2022,** *144*, 109505. https://doi.org/10.1016/j.ecolind.2022.109505
8. Zhou, M.; Li.; X.; Zhang, M.; Liu, B.; Zhang, Y.; Gao, Yu; Ullah, H., Peng, L., He, A., Yu, H. Water quality in a worldwide coal mining city: A scenario in water chemistry and health risks exploration. *Journal of Geochemical Exploration*. **2020**, *213*, 106513. https://doi.org/10.1016/j.gexplo.2020.106513
9. Gonah, T. Impact of Acid Mine Drainage on Water Resources in South Africa. In: Mujuru, M.; Mutanga, S. (eds.) *Management and Mitigation of Acid Mine Drainage in South Africa: Input for Mineral Beneficiation in Africa.* Africa Institute of South Africa, **2016**. *Project MUSE* muse.jhu.edu/book/50491. 41-65. DOI: 10.2307/j.ctvh8r359.11
10. Jhariya, D.; Khan, R.; Thakur, G.S. Impact of Mining Activity on Water Resources: An Overview Study. *Conference: National Seminar on Recent Practices and Innovations in Mining Industry* **2016**, 271 – 277.
11. Environmental Law Alliance Worldwide (ELAW). *Guidebook for evaluating mining project EIAs*. Eugene: Environmental Law Alliance Worldwide, **2010**.
12. Duruibe, J.O.; Ogwuegbu, M.O.C.; Egwurugwu, J.N. Heavy metal pollution and human biotoxic effects. *International Journal of Physical Sciences* **2007**, *2(5)*, 112-118. https://doi.org/10.5897/IJPS.9000289
13. Nunoo, S., Manu, J., Owusu-Akyaw, F.K.B., Nyame, F.K., Impact of artisanal small-scale (gold and diamond) mining activities on the Offin, Oda and Pra rivers in Southern Ghana, West Africa: A scientific response to public concern, *Heliyon*. **2022** https://doi.org/10.1016/j.heliyon.2022.e12323.
14. Galli, N.; Chiarelli, D.D.; D'Angelo, M.; Rulli, M.C. Socio-environmental impacts of diamond mining areas in the Democratic Republic of Congo. *Science of The Total Environment* **2022**, *810*, 152037. https://doi.org/10.1016/j.scitotenv.2021.152037
15. Wilson, S.A. Measuring the effectiveness of corporate social responsibility initiatives in diamond mining areas of Sierra Leone. *Resources Policy* **2022**. 77, 102651. https://doi.org/10.1016/j.resourpol.2022.102651
16. Engwicht, N.; Ankenbrand, C. Natural resource sector reform and human security in post-conflict societies: Insights from diamond mining in Sierra Leone. *The Extractive Industries and Society* **2021**, *8(4)*, 100988. https://doi.org/10.1016/j.exis.2021.100988
17. Makhetha, E.; Maliehe, S.A. "A concealed economy": Artisanal diamond mining in Butha-Buthe district, Lesotho. *The Extractive Industries and Society* **2020**, 7(3), 975-981. https://doi.org/10.1016/j.exis.2020.06.010

18. Malov, A.I. Transformation of the chemical composition of surface waters in the area of the exploited Lomonosov diamond deposit (NW Russia). *Environmental Science and Pollution Research* **2018**, *25(3)*, 33620–33636. https://doi.org/10.1007/s11356-018-3308-0
19. Yakovlev, E.Yu.; Malov, A.I.; Druzhinin, S.V.; Zykov, S.B.; Malkov, A.V.; Bedrina, D.D. Heavy metals distribution and environmental risk assessment in river sediments in the area of the Lomonosov diamond deposit (NW Russia). *Environmental Science and Pollution Research* **2020**, *27*, 35392–35415. https://doi.org/10.1007/s11356-020-09809-7
20. Malov, A.I. The role of exogenic groundwaters in kimberlite formations. *Doklady Earth Sciences* **2004**, *395–3*, 453–455.
21. Kalyuzhin, S.M. *Atlantic Salmon of the White Sea: Problems of Reproduction and Exploitation*; PetroPress: Petrozavodsk, Russia, 2003, 264. (In Russian)
22. Bondareva, L.; Fedorova, N. The effect of humic substances on metal migration at the border of sediment and water flow. *Environmental Research* **2020**, *190*, 109985. https://doi.org/10.1016/j.envres.2020.109985
23. Faisal, A.A.H.; Abdul-Kareem, M.B.; Mohammed, A.K.; Naushad, M.; Ghfar, A.A.; Ahamad, T. Humic acid coated sand as a novel sorbent in permeable reactive barrier for environmental remediation of groundwater polluted with copper and cadmium ions**.** *Journal of Water Process Engineering* **2020**, *36*, 101373. https://doi.org/10.1016/j.jwpe.2020.101373
24. Savichev, O.; Soldatova, E.; Rudmin, M.; Mazurov, A. Geochemical barriers in oligotrophic peat bog (Western Siberia). *Applied Geochemistry* **2020**, *113*, 104519. https://doi.org/10.1016/j.apgeochem.2019.104519
25. Malov, A.I.; Sidkina, E.S.; Mironenko, M.V.; Tyshov, A.S.; Cherkasova, E.V. Modeling Changes in the Composition of River Water with Discharged Wastewater: A Case Study in NW Russia. *Water* **2022**, *14*, 165. https://doi.org/10.3390/w14020165
26. Shvarov, Yu.V. Algorithmization of the Numeric Equilibrium Modeling of Dynamic Geochemical Processes. *Geochemistry International* **1999**, *37(6)*, 571–576.
27. Krainov S.R. (ed.) Methods of geochemical modeling and forecasting in hydrogeology. Moscow: Nedra, **1988**. (in Russian)
28. Varshal, G.M.; Inzkirveli, I.S.; Sirotkina, I.S.; Kolosov, I.V.; Kosheeva I.Ya. About association of fulvic acids in water solutions. *Geokhimiya* **1975**, *10*, 1581–1585. (In Russian)
29. Varshal, G.M.; Koshcheeva, I.Ya.; Sirotkina, I.S. Study of organic substances of surface waters and their interaction with metal ions. *Geokhimiya* **1979**, *4*, 598-607. (In Russian)
30. Varshal, G.M.; Velyukhanova, T.K.; Koshcheeva, I.Ya.; Dorofeeva, V.A.; Buachidze, N.S.; Kasimova, O.G.; Makharadze, G.A. Investigation of chemical forms of elements in surface waters. *Journal of Analytical Chemistry* **1983**, *38(9)*, 1590-1600. (In Russian)
31. Varshal, G.M.; Velyukhanova, T.K.; Kosheeva, I.Ya.; Kubrakova, I.V.; Baranova, N.N. Complexation of noble metals with fulvic acids of natural waters and geochemical role of these processes. In: Ermakov, A.N. (ed.) *Analytical chemistry of rare elements.* Moscow: Nauka, **1988**. 112–146. (In Russian)
32. Lipatnikova, O.A.; Grichuk D.V. Thermodynamic modeling of migration forms of heavy metals in bottom sediments on the example of Ivan'kovskoye reservoir. *Moscow University Geology Bulletin* **2011**, *2*, 5–59. (In Russian)
33. Mantoura, R.F.C.; Dickson, A.; Riley S.P. The complexation of metals with humic materials in natural waters. *Estuarine and Coastal Marine Science* **1978**, *6*, 387–408.
34. Krasinzeva, V.V.; Grichuk, D.V.; Romanova, G.I.; Kadukin A.I. Migration and occurrence forms of chemical elements in pore waters of bottom sediments in Ivankovskoe reservoir. *Geokhimiya* **1982**, *9*, 1342–1354. (In Russian)
35. Yamamoto, Y.; Kita, F.; Isono, N.; Imai, S. Impact of competitive Fe(III) ion on the complexation of humic acid and toxic metal ions. *The Japan Society for Analytical Chemistry* **2017**, *66(12)*, 875–883.
36. Guy, R.D.; Charabarti, C.L. Studies of metal-organic interactions in model systems pertaining to naturals water. *Canadian Journal of Chemistry* **1976**, *54(16)*, 2600–2611.
37. Stevenson, F.J. Stability constants of Cu^{2+}, Pb^{2+} and Cd^{2+} complexes with humic acids. *Soil Science Society of America Journal* **1976**, *40(5)*, 665–672.
38. Samadfam M., Niitsu Y., Sato S., Ohashi H. Complexation thermodynamics of Sr (II) and humic acid. *Radiochimica Acta* **1996**, *73*, 211–216.
39. Catrouillet, C.; Davranche, M., Dia, A.; Bouhnik-Le Coz, M.; Marsac, R.; Pourret, O.; Gruau, G. Geochemical modeling of Fe(II) binding to humic and fulvic acids. *Chemical Geology* **2014**, *372*, 109–118. https://doi.org/10.1016/j.chemgeo.2014.02.019
40. Lepokurova, O.E.; Trifonov, N.S.; Domrocheva, E.V. Migration forms of basic ions in groundwater of coal-bearing sediments of Kuzbass with a focus on compounds with humic acids (by simulation results). *Bulletin of the Tomsk Polytechnic University. Geo Assets Engineering* **2022**, *332(3)*, 76-89.

41. Konyshev, A.A.; Sidkina, E.S.; Cherkasova, E.V.; Mironenko, M.V.; Gridasov, A.G.; Zhilkina, A.V.; Bugaev, I.A. Migration forms of heavy metals and chemical composition of surface waters in the "Arsenic" shaft area (Pitkäranta Ore District, South Karelia). *Geochemistry International* **2020**, *58*, 1068–1074. https://doi.org/10.1134/S0016702920090050.
42. Moiseenko, T.I., Dinu, M.I., Gashkina, N.A., Kremleva, T. A. Occurrence forms of metals in natural waters depending on water chemistry. *Water Resources* **2013**, *40*, 407–416. https://doi.org/10.1134/S009780781304009X
43. Krainov, S.R.; Ryzhenko, B.N.; Shvets, V.M. Geochemistry of Groundwater. Fundamental, Applied and Environmental Aspects.Moskow: CenterLitNefteGaz, **2012**. (In Russian)
44. Malov, A.I.; Sidkina, E.S.; Ryzhenko, B.N. Model of the Lomonosov diamond deposit as a water–rock system: Migration Species, Groundwater Saturation with Rock-Forming and Ore Minerals, and Ecological Assessment of Water Quality. *Geochemistry International* **2017** *55*, 1118–1130. https://doi.org/10.1134/S0016702917090038.